



LUND UNIVERSITY

Modelling of Finger-Joint Failure in Glued

Laminated Timber Beams

Serrano, Erik; Gustafsson, Per-Johan; Larsen, Hans Jörgen

2000

Document Version:

Förlagets slutgiltiga version

[Link to publication](#)

Citation for published version (APA):

Serrano, E., Gustafsson, P.-J., & Larsen, H. J. (2000). *Modelling of Finger-Joint Failure in Glued: Laminated Timber Beams*. (TVSM-3000; Nr TVSM-3040). Division of Structural Mechanics, LTH.

Total number of authors:

3

General rights

Unless other specific re-use rights are stated the following general rights apply:

Copyright and moral rights for the publications made accessible in the public portal are retained by the authors and/or other copyright owners and it is a condition of accessing publications that users recognise and abide by the legal requirements associated with these rights.

- Users may download and print one copy of any publication from the public portal for the purpose of private study or research.
- You may not further distribute the material or use it for any profit-making activity or commercial gain
- You may freely distribute the URL identifying the publication in the public portal

Read more about Creative commons licenses: <https://creativecommons.org/licenses/>

Take down policy

If you believe that this document breaches copyright please contact us providing details, and we will remove access to the work immediately and investigate your claim.

LUND UNIVERSITY

PO Box 117
221 00 Lund
+46 46-222 00 00



LUND
UNIVERSITY

MODELLING OF FINGER-JOINT FAILURE IN GLUED-LAMINATED TIMBER BEAMS

ERIK SERRANO, PER JOHAN GUSTAFSSON
and HANS JÖRGEN LARSEN

Department
of
Mechanics
and
Materials

Structural Mechanics

MODELLING OF FINGER-JOINT FAILURE IN GLUED-LAMINATED TIMBER BEAMS

Submitted for publication in ASCE - Journal of Structural Engineering

ERIK SERRANO, PER JOHAN GUSTAFSSON
and HANS JÖRGEN LARSEN

Printed by KFS i Lund AB, Lund, Sweden, 2000.

For information, address:

Division of Structural Mechanics, LTH, Lund University, Box 118, SE-221 00 Lund, Sweden.

Homepage: <http://www.byggmek.lth.se>

Modelling of Finger-joint Failure in Glued-laminated Timber Beams

Erik Serrano, Per Johan Gustafsson and Hans Jørgen Larsen

Division of Structural Mechanics, Lund University

PO Box 118, SE-221 00 Lund, Sweden

Submitted for publication in ASCE – Journal of Structural Engineering

Abstract This paper presents a novel approach to the modelling of failure of finger-joints in glued-laminated beams. A nonlinear strain-softening model with stochastic material parameters was used to characterise the failure zone of the finger-joint. Monte Carlo simulations of the behaviour of finger-jointed laminations and of laminated beams were performed using the finite element method. Various lamination thicknesses and beam depths were investigated, as well as the effect of varying the ductility of the finger-joint. Finally the use of simplified finger-joint material models was also investigated. The results show that the proposed approach can account for such phenomena as the size effect and the laminating effect. Another observation is that the finger-joint ductility has a major influence on the lamination and beam strength and that a special case of the present modelling approach can be made to coincide with the classic weakest link theory of Weibull.

Keywords: laminated wood, glued-laminated timber, finger-joint, laminating effect, size effect, tensile strength, bending strength, finite element analysis

1 Introduction

1.1 Background

The present study is part of a research project dealing with the properties of finger-joints and laminated wood products. The overall aim of this research project is to contribute knowledge and methods to the rational modelling, analysis and prediction of the strength of glued-laminated timber (glulam).

To predict the strength properties of glulam two methods are, in principle, possible:

- testing of a number of glulam members, using a sample size sufficiently large to determine the properties on a statistical basis
- using a model, verified by testing, linking the properties of the glulam to the properties of the individual laminations.

Taking into account the many parameters influencing the properties of glulam - e.g. timber species and grade, lamination thickness, the properties of finger-joints, member depth - and the number of specimens needed, the former method is clearly too expensive as a general method. A model which makes it possible to estimate the properties of glulam from those of the laminations is therefore desirable. In addition, a rational model adds to the understanding of glulam behaviour.

1.2 Previous Work

Several models to predict the behaviour of glulam have been proposed by e.g. Foschi and Barrett (1980), Ehlbeck et al. (1985) and Colling (1990) – known as the “Karlsruhe model”, Hernandez et al. (1989), Nestic et al. (1994), Faye et al. (1996) and Renaudin (1997). All these models, except those of Hernandez et al. and Nestic et al., are based on a subdivision of the glulam member into elements, frequently standard finite elements. Loading is applied to the beam, and the stresses in all the elements are evaluated. This is done for the centroid of the element, each element having the same height as the lamination. The models of Hernandez et al. and Nestic et al. use transformed section methods (based on beam theory) to calculate the stresses at the mid-depth of each lamination, to determine the ultimate load-bearing capacity of the beam. This means that in all models the stress at mid-depth of a lamination is used as a measure of the risk of failure.

The original model of Foschi and Barrett was based on a brittle stress criterion, i.e. when the stress in the most stressed element was equal to the strength the beam was considered to have no load-bearing capacity left. Later models introduced the nonlinearities in compression and accounted for stress redistribution when an element failed in tension: failed elements were removed, and the beam response re-calculated.

In the Karlsruhe model, the finger-joints are assumed to be brittle and failure in a finger-joint means failure of the entire beam. For tensile failure in the wood, the surrounding elements are assumed to take up the released stresses.

In the model proposed by Renaudin, the failure of an element results in redistribution of stresses to neighbouring elements, following explicit rules that have been set up using finite element analyses of the stress distributions in the vicinity of the cracks resulting from the failure.

Although a locally brittle response of the material in tension is assumed in all the above models, the assumption of redistribution of stresses after failure introduces a considerable amount of ductility in the model at a global level.

In Serrano (1997) an experimental and numerical investigation on the behaviour of finger-joints is presented. It was found that it is possible to simulate the strain-softening behaviour of a finger-joint in pure tension. It was also found that a brittle and apparently linear elastic behaviour, from a global point of view, was strongly influenced by the local nonlinear behaviour of the bond line.

In Serrano and Larsen (1999), using both linear elastic fracture mechanics and nonlinear fracture mechanics, the behaviour of a beam after failure in the outer lamination was studied. It was assumed that a crack is formed at the failed section in the glue line between the outer and the second lamination, and the condition for that crack being stable, which is a condition for redistribution of stresses, was investigated. A stable crack propagation along the outer lamination can take place, but only for small lamination thicknesses, typically less than 10 mm. A series of linear elastic finite element analyses also showed that commonly made assumptions regarding the stress distribution in glulam beams are not always true. A beam loaded in pure bending was simulated. In the outer lamination on the tension side it was assumed to be a zone having a lower stiffness than the rest of the beam. The influence of the length of this low-stiffness zone was investigated. As an example, it was found that for a small length of this zone (30 mm) the mean stress in the outer lamination was only reduced by 3% for a 25% stiffness reduction.

The properties of the outer laminations, especially the strength of the finger joints, are very important for the modelling of glulam. Using as a failure criterion the fact that the mid-depth stress in the outer lamination corresponds to the tensile strength of the lamination, defined as the average stress at failure in a uni-axial tension test, is far too primitive.

This is one of the reasons why the theoretical models are not used in practice to determine the properties of glulam. Instead, semi-empirical models, e.g. the one proposed in Schickhofer (1996), are used. They are, however, only valid within a small parameter range.

In the following, a more detailed modelling of the finger-joint failure in a glulam beam is described. In principle, it is possible to use the same type of approach for the failure of the wood or the bond line between the laminations.

2 Present Study

2.1 Aim

The aim of the present study is:

- to set up a detailed model of a finger-joint, using an approach based on non-linear fracture mechanics (NLFM) and assuming that the material parameters are stochastic, and
- to use the finger-joint model in finite element simulations, and investigate behaviour of the finger-joint and laminated beams in terms of a) size effect, b) depth effect, c) laminating effect and d) effect of finger-joint ductility.

2.2 Model Description

Wood is known to be a material with highly variable properties and several options to model the wood material and the finger-joints exist: deterministic or stochastic models which in turn can be linear, nonlinear or perfectly plastic to account for plasticity, damage or crack formation. For the finger-joints a rigid model could also be used. Different possibilities of modelling the stress-deformation properties of a finger-joint are shown schematically in Fig. 1.

In the models taking the variability into account, the stochastic parameters can be correlated or not. The types A, B and D can be regarded as different special cases of C, and the deterministic modelling as a special case of stochastic modelling.

Since the present study emphasizes the behaviour of the finger-joints, the wood outside the finger-joint is modelled as a linear elastic, orthotropic and homogeneous material with deterministic properties. The bondline bonding the outer tension lamination of a beam to the next lamination acts in all cases studied as a linear elastic layer with deterministic properties, although the bondline model is nonlinear.

The finger-joint is modelled with a number of parallel nonlinear spring elements of initial zero length, see Fig. 2. Due to the zero initial length, the elongation of such a spring is associated with crack formation and represents the local additional deformation due to the presence of the finger-joint. Each spring is assumed to represent the response of a finger-joint area defined by the lamination width times the distance between neighbouring nodes in the height direction of the lamination. The present modelling is thus closely related to a so called fictitious crack model, a fracture mechanics model

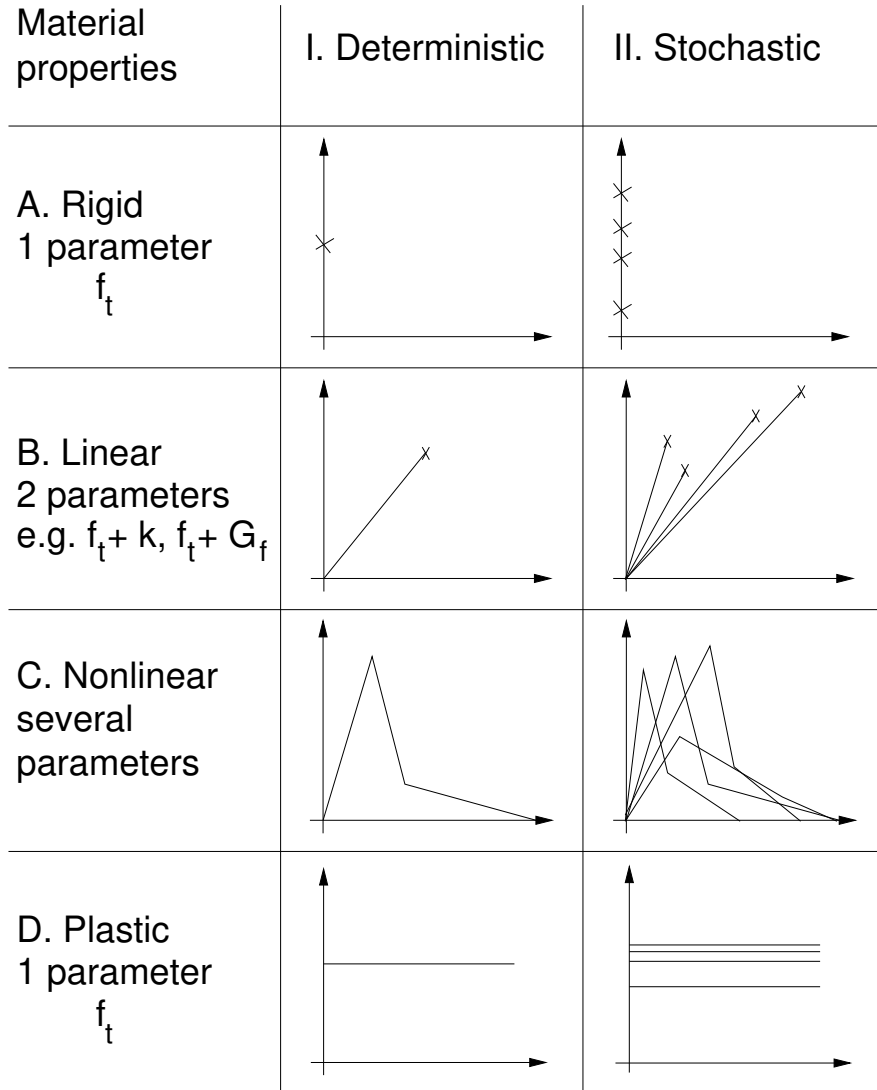


Figure 1: Different approaches of modelling the stress vs. the deformation response of a finger-joint. f_t is the strength, k is the stiffness and G_f is the fracture energy.

for describing the gradual localised damage of a material, (Hillerborg et al. (1976), Gustafsson (1985)).

The finger-joint spring characteristics are chosen in line with results from tests and elaborated wide face FE-modelling of finger-joints (Serrano 1997), see Fig. 2a, taking into account the finger geometry and the nonlinear bond-line performance. The nonlinear responses of the finger-joint springs are described by piecewise linear relations, see Fig. 3, and it is assumed that the stress-elongation relations are linear up to failure. The finger-joint springs are characterised by strength, elongation at failure and the shape of the force-elongation curve. The strength and the elongation at failure are both described by an average value and a coefficient of variation (COV). Furthermore it is assumed that these variables are spatially uncorrelated. The present modelling of the finger-joint thus corresponds to a modelling of type C in Fig. 1.

The present study primarily concerns the bending strength of laminated beams of different height and with different lamination thicknesses, with a finger-joint located in the outer tension lamination. The beams are subjected to pure bending and analysed using the finite element method.

2.3 Finite Element Implementation

FE-model

In the finite element models, plane stress conditions are assumed, and due to symmetry only one half of the beam is modelled. The finger-joint is located in the symmetry plane, resulting in the finger-joint nonlinear springs acting in pure tension. The total length of the beam is set to be 1 m, which is enough to avoid boundary effects of the loading which is imposed by rotating the end sections of the beam. The end sections are assumed to remain plane during deformation. The total number of elements are 3900–5700 and the number of nodes are 4100–6000 for the different beam sizes. An example of the FE-mesh used for the beam height, h , being 450 mm and the lamination thickness, t , being 45 mm is shown in Fig. 4.

Input Data

The wood is treated as a linear elastic orthotropic material with $E_x = 16800$ MPa, $E_y = E_x/30 = 560$ MPa, $G_{xy} = E_x/16 = 1050$ MPa, $\nu_{xy} = 0.45$. Here x denotes the fibre direction which is assumed to coincide with the beam axis. The value of E_x was taken from an investigation by Serrano (1997).

The bondline of the outer tension lamination is modelled with nonlinear

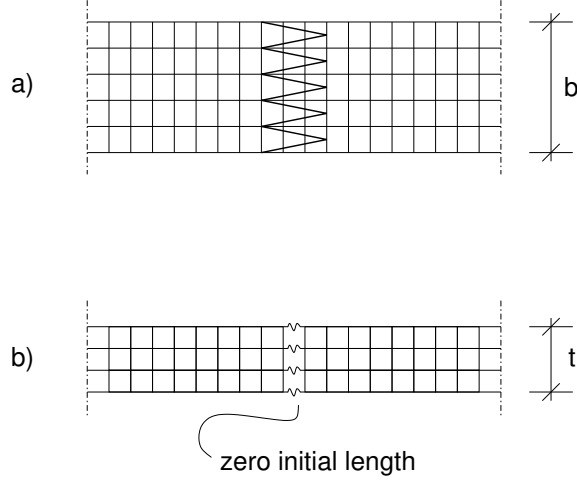


Figure 2: Schematic of finger-joint and FE-modelling used in a) Serrano (1997) and b) in the present study.

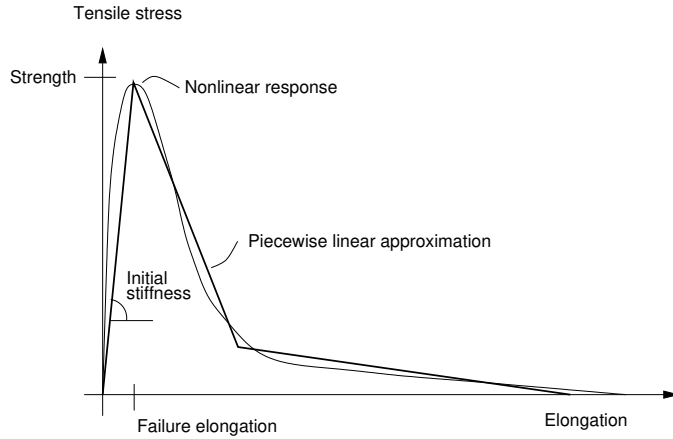


Figure 3: Nonlinear stress-elongation response of a finger-joint and a piecewise linear approximation.

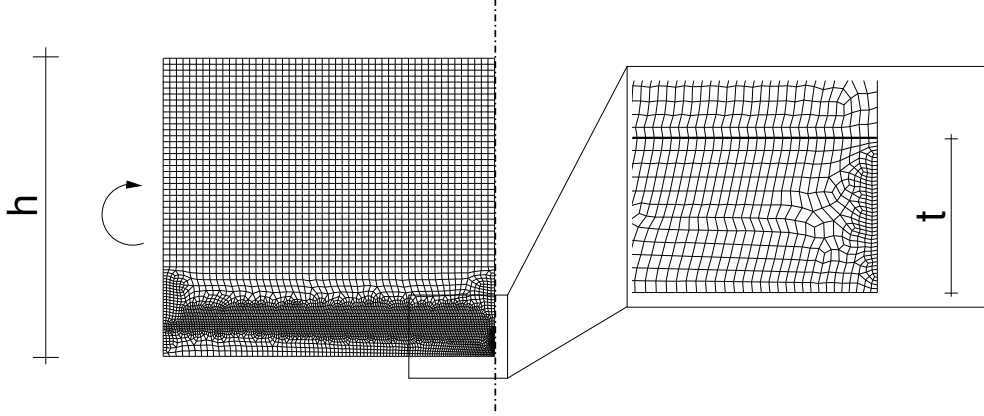


Figure 4: FE-mesh used for beams with $h = 450$ mm and $t = 45$ mm.

bondline elements, Serrano and Larsen (1999). However, for all cases the stresses in this bondline are within the elastic region.

To calibrate the input data of the nonlinear springs, test results from tensile tests on 10 mm thick finger-jointed laminations were used (Serrano 1997). These tests were performed on different adhesive types and only three nominally equal tests were made, so that the variability in strength could not be estimated from this test series. From this test series, finger-joints glued with a resorcinol-phenol adhesive were chosen for the calibration. Their mean strength was approximately 55 MPa.

The shape of the force-elongation curves of the springs was set to be according to Fig. 5, which is in line with the results reported in Serrano (1997). Using this shape it is possible to determine the spring response in terms of two parameters only, the strength and the failure elongation, f_{t0} and δ_0 respectively.

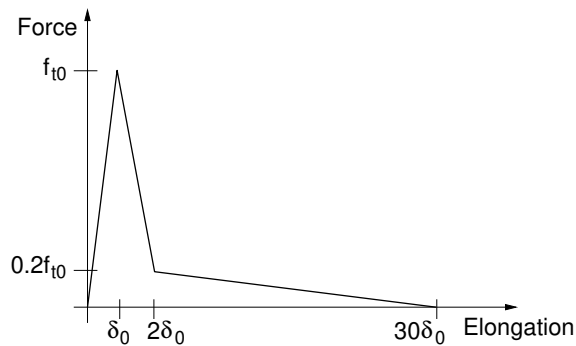


Figure 5: Nonlinear force-elongation response of a finger-joint spring element.

The calibration of input data was performed in an iterative manner. Initially it was assumed that the failure elongation of the springs was deterministic and equal to $\delta_0 = 0.02$ mm. Assuming furthermore a log-normal distribution for the strength f_{t0} , the mean value, denoted \bar{f}_{t0} , and the COV were then varied in a number of FE-simulation series, each consisting of 1000 simulations, until the mean tensile strength of the lamination was close to 55 MPa (same as above), and the COV of the tensile strength 15% (chosen). This was achieved for $\bar{f}_{t0} = 82$ MPa and a COV of 40%. Following this the failure elongation was also assumed to be a log-normal distributed stochastic variable, uncorrelated with the strength and with a mean value of $\bar{\delta}_0 = 0.02$ mm and a COV equal to 40%. New simulation series were performed, changing the mean strength and the COV of strength, until the mean and COV of strength of the lamination again were 55 MPa and 15% respectively. This was finally achieved for the values of $\bar{f}_{t0} = 80$ MPa with a COV of 30%.

The above reported calibrated values of strength apply to the inner parts of a lamination, where each nonlinear spring represents a finger-joint area of $b \times 1.125$ mm². Here b is the width of the beam and the 1.125 mm represent the distance between the nodes along the symmetry plane. Since the edge springs represent only half of this area, it is reasonable to give them a higher strength value. This was done according to the weakest link theory of Weibull (1939), using the 2-parameter Weibull distribution. For the present values of $\bar{f}_{t0} = 80$ with a COV of 30%, this means that the edge springs were given an approximately 20% larger value of \bar{f}_{t0} . The calibrated values are given in Table 1.

Table 1: Calibrated spring characteristics. Log-normal distribution.

| Parameter | Mean | COV |
|----------------|----------|-----|
| $f_{t0,inner}$ | 80.0 MPa | 30% |
| $f_{t0,edge}$ | 96.4 MPa | 30% |
| δ_0 | 0.02 mm | 40% |

3 Results

3.1 General Remarks

The finite element simulations performed involve four major simulation series:

1. Bending strength of laminated beams. Three different heights, $h=135$, 450 and 900 mm and two different lamination thicknesses $t=33$ and 45 mm.
2. Pure tension of laminations with thickness $t=10$, 33 and 45 mm.
3. The effect of finger-joint ductility on the bending strength.
4. The effect of using a simplified finger-joint material model.

The results from the finite element simulations are presented with a mean value and a corresponding 95%-confidence interval of the mean value, lower 5%-fractile values and the COV. The bending strength is estimated using the ultimate bending moment from the finite element simulations and assuming ordinary beam theory to be valid. The fractile values given are distribution-free estimates. All strength statistics are based on 1000 simulations.

From the results of simulation series 1 and 2, different factors relating to the strength of glulam beams and laminations are calculated. Since these factors are inconsistently defined in literature, the definitions used here are given:

Size effect For a structure of fixed geometrical shape, the effect that the strength, as evaluated in terms of force/unit area, diminishes at an increasing size. For a glulam beam, the fixed geometrical shape means that the lamination thickness increases with increasing beam depth.

Depth factor (in bending) For a beam in bending, the effect that the strength diminishes at an increasing depth. The other geometric parameters are kept constant, e.g. lamination thickness.

Laminating effect The effect that the strength of a lamination increases when contained in a beam. Also the effect that the strength increases for a beam in bending at decreasing lamination thicknesses.

3.2 Bending Strength and Tensile Strength

In Table 2, the bending strength statistics are given for the beam geometries investigated. Three different beam depths, h , and two different lamination thicknesses, t , were investigated.

The greater the depth of the beam, the closer the state of pure tensile stress is achieved in the outer lamination. Therefore, for comparison with the beam bending results, a series of simulations was performed involving pure tension of laminations, 33 and 45 mm thick. These results are summarised in Table 3. For comparison, the results from the calibration procedure are also given here.

Table 2: Bending strength statistics.

| h (mm) | t (mm) | Mean (MPa) | 5% (MPa) | COV (%) |
|-------------|-------------|---------------|-------------|------------|
| 135 | 45 | 58.4±0.5 | 44.6 | 14 |
| 450 | 45 | 51.5±0.4 | 41.0 | 12 |
| 900 | 45 | 49.5±0.4 | 39.6 | 12 |
| 135 | 33 | 58.6±0.5 | 44.7 | 14 |
| 450 | 33 | 52.3±0.4 | 41.3 | 12 |
| 900 | 33 | 50.8±0.4 | 40.4 | 12 |

Table 3: Tensile strength statistics.

| $h = t$ (mm) | Mean (MPa) | 5% (MPa) | COV (%) |
|-----------------|---------------|-------------|------------|
| 10 | 55.4±0.5 | 41.8 | 15 |
| 33 | 48.3±0.4 | 38.5 | 12 |
| 45 | 46.8±0.3 | 38.1 | 12 |

3.3 Effect of Size, Depth and Lamination Thickness

From the results reported above, it is possible to derive a number of factors related to the strength of the laminations and beams as a function of size, depth and of the lamination thickness according to the definitions above.

Size Effect for Lamination in Tension

The size effect found for the different lamination thicknesses in pure tension is shown in Fig. 6. The curves represent least square fits of a power relation according to:

$$f_t = f_{t0} \left(\frac{t}{1.125} \right)^{-\beta} \quad (1)$$

where f_t is the tensile strength of a lamination of thickness t mm and f_{t0} is the strength of the reference area of the finger-joint, i.e. the strength of the nonlinear spring. It is evident that the present model gives a size effect that is less pronounced at the 5%-fractile level than at the mean value level.

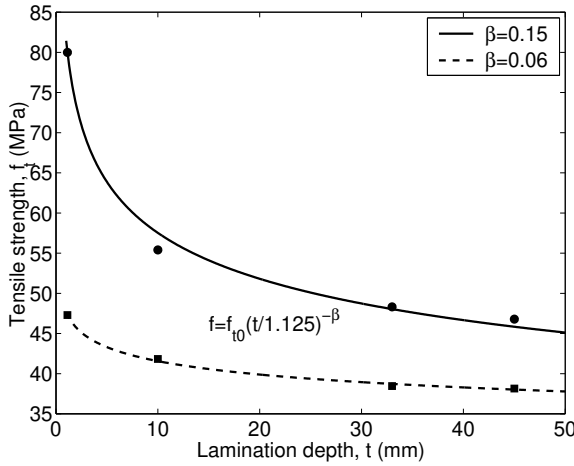


Figure 6: Size effect in pure tension. The solid line and dots represent mean values and the dashed line and squares represent 5%-fractile values.

Depth Effect for Beam in Bending

The depth factors calculated are relative bending strengths, with the strength of a beam with $h = 600$ mm and $t = 45$ mm as reference. This beam depth was not simulated in the present study, and the strength values of this beam were computed using linear interpolation. The reason for using $h = 600$ mm as reference is that this is also used in the present European code which states that a depth factor k_h should be used for beam depths h less than 600 mm. k_h is given by:

$$k_h = \min \left\{ \begin{array}{l} \left(\frac{600}{h} \right)^{0.2} \\ 1.15 \end{array} \right. \quad (2)$$

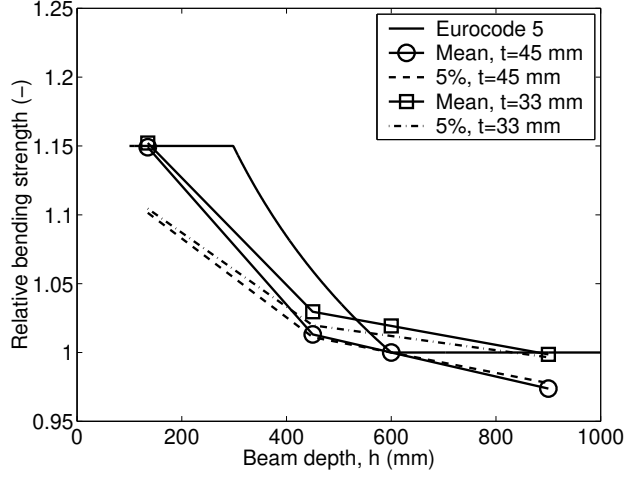


Figure 7: Relative bending strength (depth factors).

The relative strengths are given in Fig. 7 which shows that the depth factor is different for the mean values as compared to the characteristic values, and that the depth factor depends on the lamination thickness.

Laminating Effect

The apparent strength increase of laminations when contained in beams of different depths was calculated and the results are given in Fig. 8. Here the strength increase is defined as the ratio of beam bending strength to single lamination tensile strength.

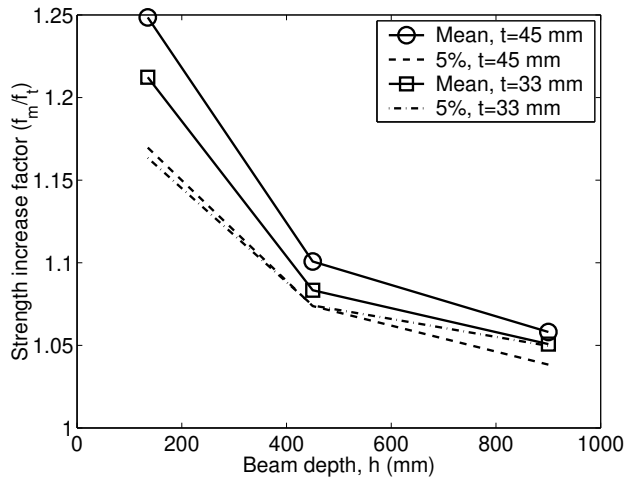


Figure 8: Strength increase factors.

Finally the laminating effect due to the use of thinner laminations is given in Table 4. Here the bending strength of a beam with $t = 45$ mm is compared with a beam having a lamination thickness of $t = 33$ mm.

Table 4: Relative bending strength for thinner laminations ($f_{t=33}/f_{t=45}$).

| h (mm) | Mean (MPa) | 5% (MPa) |
|-----------|---------------|-------------|
| 135 | 1.00 | 1.00 |
| 450 | 1.02 | 1.01 |
| 900 | 1.03 | 1.02 |

3.4 Influence of Finger-joint Ductility

A series of simulations was performed to investigate the influence of the finger-joint ductility on the tensile strength of a lamination. Here the ductility of the finger-joint is defined by its fracture energy, which is equal to the area under the stress-elongation curve. This fracture energy is equal to the energy required to fully separate a unit area of the finger-joint. The different ductilities were simulated by changing the positions of the breakpoints, δ_0 , of the piecewise linear response of the nonlinear springs, cf. Fig. 5. Two different approaches were tested, one where all three breakpoints were changed and one where the initial stiffness was unchanged. Changing all the breakpoint positions results in a change of the initial stiffness of the springs so that the ratio of the spring stiffness to the wood stiffness will be different for different values of the fracture energy. This results in turn in different linear elastic stress distributions for different fracture energy values. However, keeping the initial stiffness of each spring constant gives as a result that the linear elastic stress distributions are equal irrespective of the fracture energy. Therefore, for this case there exists a minimum mean tensile strength of the lamination which is the one obtained for the case of a weakest link failure.

The mean fracture energy of the springs was for the reference case $G_f = 6.4$ kJ/m² and the different simulations represent fracture energies of this value multiplied by factors varying between 0.125 and 8. The case of pure tension of a 45 mm thick lamination was investigated and the results are presented in Fig. 9, showing the mean values and error bars corresponding to 95% confidence intervals. The solid line represents the results when all breakpoints of the stress-elongation curve are changed and the dashed line represents the case with the initial stiffness kept constant.

Fig. 9, dashed line, shows that the reference case ($G_f = 6.4 \text{ kJ/m}^2$) almost coincides with a weakest link failure, since the tensile strength diminishes very little for smaller values of fracture energy.

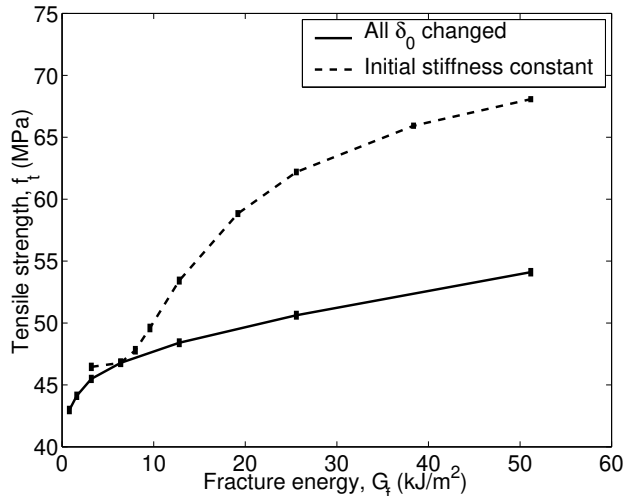


Figure 9: Influence of fracture energy on tensile strength. $t=45 \text{ mm}$.

3.5 Influence of the Finger-joint Model

The finger-joint model presented above uses a nonlinear fracture mechanics approach with two stochastic variables to characterise the finger-joint “material”. The strength and the failure elongation of the nonlinear spring elements were assumed to be uncorrelated. Here a simplified description of the finger-joint with only one stochastic variable will be used instead. The strength of the finger-joint is considered to be the only stochastic variable and the failure elongation depends on this. Two extreme cases of such dependence are shown in Fig. 10. The previously used concept of two stochastic variables is shown together with two alternative models, equal stiffness and equal failure elongation.

In the case of equal stiffness, the failure elongation is fully correlated with the strength. In the case of equal failure elongation, the initial stiffness is instead fully correlated with the strength. It turns out that the equal stiffness model results in a state of deformation which is very close to the one predicted by ordinary beam theory. Furthermore, since the failure of the beam is brittle and occurs at the instant of failure of the first nonlinear spring (weakest link failure), simple linear elastic beam theory analyses give the same results as the finite element simulations. If the input of the model

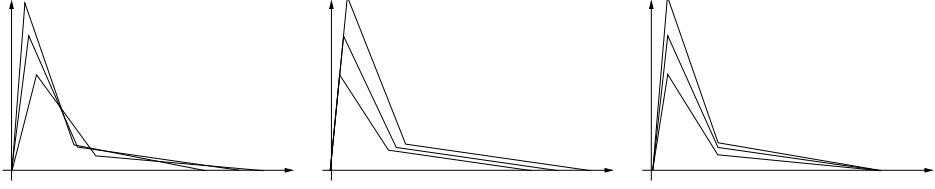


Figure 10: Left: The model with two stochastic variables, Center: Equal stiffness, Right: Equal failure elongation

in terms of strength of the nonlinear springs is assumed to be from a Weibull distribution, analytical solutions exist and no Monte-Carlo simulations have to be performed. For this case the present model coincides with the classic Weibull weakest link theory.

To compare different models, a calibration of input data according to the method described earlier was performed. In an iterative manner the mean strength of the nonlinear springs was changed until the strength statistics of the 10 mm lamination was the same as previously reported (mean 55 MPa and COV 15%). For both models the strength was assumed to be log-normally distributed. The calibrated values of strength are $\bar{f}_{t0} = 82\text{MPa}$ with COV=26% for the equal stiffness model and $\bar{f}_{t0} = 82\text{MPa}$ with COV=40% for the equal failure elongation model. The bending strength statistics using the two models are summarised in Table 5. In the simulations using the equal stiffness model, ordinary beam theory was used.

Table 5: Bending and tensile strength statistics using models with one stochastic variable.

| h (mm) | t (mm) | Eq. stiffness | | | Eq. failure elong. | | |
|-------------|-------------|---------------|-------------|------------|--------------------|-------------|------------|
| | | Mean (MPa) | 5% (MPa) | COV (%) | Mean (MPa) | 5% (MPa) | COV (%) |
| 135 | 45 | 57.5 | 43.5 | 14 | 61.0 | 49.6 | 11 |
| 450 | 45 | 50.5 | 40.0 | 12 | 55.3 | 46.9 | 9 |
| 900 | 45 | 48.4 | 38.8 | 12 | 53.4 | 46.1 | 8 |
| 10 | 10 | 55.3 | 41.4 | 15 | 54.7 | 42.3 | 15 |
| 33 | 33 | 47.8 | 37.7 | 12 | 51.2 | 43.7 | 9 |
| 45 | 45 | 46.1 | 36.8 | 12 | 50.3 | 43.2 | 8 |

4 Discussion

4.1 Bending and Tensile Strength

As expected, the beam bending strength is higher than the tensile strength of the lamination. As an example, the strength increase at 5%-fractile level of the 45 mm lamination when contained in a beam was found to be 5–20% for the beam depths examined. This is due to the fact that the outer lamination is exposed to a non-uniform stress distribution, and that when evaluating the strength of the beam, the nominal stress at the outer edge is used as a reference. The strength increase can be expressed as an equivalent position of failure in the outer lamination, if ordinary beam theory is used for evaluation. This equivalent failure position, z , measured from the outer tensile edge can be calculated according to:

$$z = \frac{h}{2} \left(\frac{f_m}{f_t} - 1 \right) \quad (3)$$

where f_m and f_t denote the bending strength of the beam and the tensile strength of a lamination, respectively, and h is the beam depth. For the case of a zero strength increase in bending, i.e. $f_m = f_t$, (3) states that the failure takes place at the outer tensile edge, $z = 0$.

For the case of the 45 mm thick lamination it is found, using (3) and the results from Fig. 8, that the failure positions are 9.8, 14.7 and 17.3 mm when the beam depth is 135, 450 and 900 mm respectively. This shows that the larger the beam depth, the closer a state of pure tension in the outer lamination is achieved, leading to the average failure position being equal to the mid-depth of the lamination, i.e. 22.5 mm for the present case. As mentioned in the introduction, a common assumption made in previous models is that this mid-depth is the characteristic point of failure initiation, independent of beam depth and lamination thickness.

4.2 Finger-joint Ductility

For the smaller values of the fracture energy the failure of the finger-joint is very brittle and occurs prior to the existence of a fully developed fracture process zone. For these cases it is the slope of the first descending part of the stress-elongation relation of the springs that determines the strength. Thus, for these cases a change in slope of the descending branch will have the same effect as a change of fracture energy. As an example, what has been presented here as a doubling of the fracture energy of the finger-joint is equivalent to

halving the negative slope of the descending part of the stress-elongation curve.

4.3 Modelling Aspects

Being closely related to a fictitious crack model, the present finger-joint modelling approach includes the brittle failure at zero fracture energy and the perfectly plastic failure as special cases. Furthermore, as opposed to a linear elastic fracture mechanics approach, it is possible to use the present approach irrespective of the presence of stress gradients.

The two extreme cases of equal stiffness or equal failure elongation of the finger-joint nonlinear springs can be seen as special cases of the more complex model with two stochastic variables. Both the equal stiffness model and the model with two stochastic variables predict reasonable results in terms of size effects and laminating effects. The equal stiffness model, however, has only been tested for the case of an extremely brittle finger-joint where ordinary beam theory could be used for the simulation. For other cases FE simulations must be performed and there is no longer any need for a simplified material model.

The equal failure elongation model results in a larger loss of variability compared with the other models. The COV of the tensile strength of a lamination changed from 15% to 8% when the lamination thickness changed from 10 to 45 mm. As a result, the size effect in tension is very small and at the characteristic level even negative, i.e. a higher tensile strength for larger sizes.

5 Conclusions

The following conclusions can be drawn from the present study:

- The finger-joint model is general in the sense that it can be used for both locally brittle and ductile materials.
- The present finger-joint model predicts a size effect, a depth effect and laminating effects.
- The COV of the bending strength was of the same magnitude as for the finger-jointed lamination, but about 40–50% of the COV of the nonlinear springs.
- The characteristic position of failure initiation in an outer lamination of a beam depends on the beam depth.
- A simplified version of the present finger-joint model can be made to coincide with the classic Weibull theory.

6 Acknowledgements

The financial support by the Swedish Council for Building Research (BFR), which made this research possible, is gratefully acknowledged.

Appendix I. References

Ehlbeck, J., Colling, F. and Görlacher, R. (1985). “Einfluß keilgezinkter lamellen auf die Biegefestigkeit von Brettschichtholzträgern. Entwicklung eines rechenmodells.” *Holz als Roh- und Werkstoff*, Vol. 43, 333–337.

Colling, F. (1990). “Tragfähigkeit von Biegeträgern aus Brettschichtholz in Abhängigkeit von den festigkeitsrelevanten Einflußgrößen.” PhD thesis, University of Karlsruhe, Germany.

Faye, C., Lac, P., and Castéra, P. (1996). “Application of SFEM to the design of glued laminated timber beams.” Paper presented at the European Workshop on Application of Statistics and Probabilities in Wood Mechanics., Bordeaux, France

Falk, R. H., Solli, K. H. and Aasheim, E. (1992). “The performance of glued laminated beams manufactured from machine stress graded Norwegian spruce.” *Rep. no. 77*. Norwegian Institute of Wood Technology, Oslo, Norway.

Foschi, R. O., and Barrett, J. D. (1980). “Glued-Laminated Beam Strength: A Model.” *J. Struct. Div.*, ASCE, 106(8), 1735–1754.

Gustafsson, P. J. (1985). “Fracture Mechanics Studies of Non-yielding Materials Like Concrete: Modelling of Tensile Fracture and Applied Strength Analyses.” PhD thesis. *Report TVBM-1007*. Division of Building Materials, Lund Institute of Technology, Lund, Sweden.

Hernandez, R., Bender, D. A., Richburg, B. A., and Kline, K. S. (1991). “Probabilistic modeling of glued-laminated timber beams.” *Wood and fiber science*, Vol. 24(3), pp. 294–306.

Hillerborg, A., Modéer, M. and Petersson, P-E. (1976). “Analysis of crack formation and crack growth in concrete by means of fracture mechanics and finite elements.” *Cement and concrete research*. Vol. 6. pp. 773–782.

Nestic, R., Milner, H. R. and Stringer, G. R. (1994). “The evaluation of glued laminated timber strength from lamination tension tests.” Paper presented at the IUFRO-S5.02/Timber Engineering meeting, Sydney, Australia.

Renaudin, P. (1997). “Approche probabiliste du comportement mecanique du bois de structure, prise en compte de la variabilite biologique.” PhD thesis. Ecole Normale Supérieure de Cachan, Paris, France.

Serrano, E. (1997). “Finger-joints for Laminated Beams. Experimental and numerical studies of mechanical behaviour.” *Report TVSM-3021*, Lund University, Division of Structural Mechanics, Lund, Sweden.

Serrano, E. and Larsen, H. J. (1999). “Numerical investigations of the laminating effect in laminated beams.” *Journal of Structural Engineering*. ASCE, 125 (7) pp. 740-745.

Schickhofer, G. (1996). “Development of efficient glued laminated timber.” *Proc., CIB-W18, Meeting 29, Bordeaux, France*, International Council for Building Research Studies and Documentation, University of Karlsruhe, Germany.

Weibull, W. (1939). “A statistical theory of the strength of materials.” *Nr. 151. Proc. Royal Swedish Institute for Engineering Research*. Stockholm, Sweden.

Appendix II. Notation

The following symbols are used in the present paper:

| | | |
|----------------|---|---|
| b | = | beam width; |
| E_x, E_y | = | moduli of elasticity in grain and across grain direction; |
| f_m | = | beam bending strength; |
| f_t, f_{t0} | = | tensile strength of lamination and of nonlinear spring; |
| \bar{f}_{t0} | = | mean tensile strength of nonlinear spring; |
| G_f | = | fracture energy; |
| G_{xy} | = | shear modulus; |
| h | = | beam depth; |
| k_h | = | depth factor; |
| t | = | lamination thickness; |
| β | = | power in size effect equation; |
| δ_0 | = | displacement at first breakpoint of a stress-elongation curve; and |
| ν_{xy} | = | Poisson’s ratio. |